Pharm Res (2020) 37: 77
https://doi.org/10.1007/s11095-020-02795-y

RESEARCH PAPER

Supersaturated-Silica Lipid Hybrids Improve in Vitro Solubilization of Abiraterone Acetate

Hayley B. Schultz [1,2] • Paul Joyce [1,2] • Nicky Thomas [1,2] • Clive A. Prestidge [1,2]

Received: 25 December 2019 / Accepted: 3 March 2020 / Published online: 31 March 2020

ABSTRACT

Purpose Abiraterone acetate (AbA) is a poorly water-soluble drug with an oral bioavailability of <10% and a significant pharmaceutical food effect. We aimed to develop a more efficient oral solid-state lipid-based formulation for AbA using a supersaturated silica-lipid hybrid (super-SLH) approach to achieve high drug loading, improve in vitro solubilization and mitigate the food effect, while gaining a mechanistic insight into how super-SLH are digested and release drug.

Methods The influence of super-SLH saturation level and lipid type on the physicochemical properties and in vitro solubilization during lipolysis of the formulations was investigated and compared to the commercial product, Zytiga.

Results Super-SLH achieved significantly greater levels of AbA solubilization compared to Zytiga. Solubilization was influenced by the AbA saturation level, which determined the solid state of AbA and the relative amount of lipid, and the lipid utilized, which determined its degree of digestion and the affinity of the lipid and digestion products to the silica. A fine balance existed between achieving high drug loads using supersaturation and improving performance using the lipid-based formulation approach. The non-supersaturated SLH prepared with Capmul PG8 mitigated the 3-fold in vitro food effect.

Conclusion SLH and super-SLH improve in vitro solubilization of AbA, remove the food effect and demonstrate potential to improve oral bioavailability in vivo.

KEY WORDS abiraterone acetate · formulation · poorly water-soluble drug · bioavailability · lipid · oral · dissolution · lipolysis

ABBREVIATIONS

^{1}H NMR	nuclear magnetic resonance
Ab	abiraterone
AbA	abiraterone acetate
AUC_{sol}	Area under the solubilisation-time curve
BCS	Biopharmaceutics Classification System
DG	Diglyceride
FA	Fatty acid
HCl	Hydrochloric acid
LBF	Lipid-based formulation
LCMS	Liquid chromatography-mass spectrometry
MG	Monoglyceride
NaOH	Sodium hydroxide
PWSDs	Poorly water-soluble drugs
SD	Standard deviation
SEM	Scanning electron microscopy
S_{eq}	Equilibrium solubility
Super-SLH	Supersaturated silica-lipid hybrid
SLH	Silica-lipid hybrid
TGA	Thermogravimetric analysis
XRPD	X-ray powder diffraction

Guest Editor: Sheng Qi

Electronic supplementary material The online version of this article (https://doi.org/10.1007/s11095-020-02795-y) contains supplementary material, which is available to authorized users.

✉ Clive A. Prestidge
clive.prestidge@unisa.edu.au

[1] University of South Australia Cancer Research Institute, Adelaide, South Australia 5000, Australia

[2] ARC Centre of Excellence in Convergent Bio-Nano Science and Technology, University of South Australia, Mawson Lakes Campus, Mawson Lakes 5095, Australia

INTRODUCTION

Poorly water-soluble drugs (PWSDs) continue to emerge from pharmaceutical discovery programs, challenging formulators to develop oral formulations with adequate performance and acceptable dose. The poor solubilization and oral bioavailability of PWSDs can be enhanced utilizing lipid-based formulations (LBF) [1]. However LBFs can be compromised by low drug loading and inherent instability. Recently, solid LBF have emerged for their ability to confer controlled release, improved stability, improved safety and industrial benefits compared to their liquid-state counterparts [2–4]. However, through solidification by the addition of a solid carrier, the drug loading is reduced, limiting their clinical application to drugs of low dose and high potency.

Supersaturated silica-lipid hybrids (super-SLH) are a solid-state LBF strategy that aims to overcome low drug loading by thermally induced supersaturation and promoting drug concentrations above the equilibrium solubility (S_{eq}) in lipids [5]. Drug supersaturated in lipid is stabilized by porous silica microparticles though imbibition into the silica pores via a capillary action [6], to form a solid super-SLH powder. Previously, the pores were shown to restrict recrystallization of the drug upon cooling, maintaining the drug in the amorphous/molecular state [5]. On oral dosing, super-SLH delivers the drug to the gut in the pre-dissolved molecular state, removing the absorption rate limiting step of dissolution. Akin to LBF, super-SLH have the potential to mimic the postprandial (food) effect, through the hydrolysis of the digestible lipids (when administered at 2 g or more) [7]. The stimulation of pancreatic and gallbladder secretions generates colloidal vesicles which can retain drug molecules in the solubilized state prior to absorption [4]. This lipidic and solubilizing environment potentially allows for more efficient absorption, independent of food. This was evidenced in a recent study were ibuprofen super-SLH (227% S_{eq}, 19.1% ***w***/w) was shown to have a 2.2-fold greater bioavailability than a commercial ibuprofen product, when orally administered to Sprague-Dawley rats [8]. Furthermore, the oral bioavailability was equivalent to the first generation SLH (non-supersaturated and fabricated by spray drying) which previously achieved 2-fold greater exposure in humans compared to the commercial product [9], yet possessed a 2.7-fold greater drug load. The application of super-SLH to other PWSDs is yet to be investigated.

Abiraterone acetate (AbA), marketed as Zytiga, is an androgen biosynthesis inhibitor indicated for the treatment of metastatic castration resistant prostate cancer [10]. AbA is an inactive prodrug which undergoes hydrolysis in the gut, enterocytes and liver to the active metabolite abiraterone (Ab). AbA possesses significant oral delivery challenges. It is a Biopharmaceutics Classification System (BCS) Class IV compound with high lipophilicity [11]. Due to these attributes, its oral bioavailability is estimated to be <10% and therefore a large daily dose of 1000 mg (four 250 mg tablets) is required to reach therapeutic blood levels. Furthermore, it must be administered in the fasted state, i.e. no consumption of food for 2 h before and 1 h after dosing. This is to avoid AbA's significant positive pharmaceutical food effect, where a low-fat meal can increase the exposure of the drug 5-fold and a high-fat meal by 10-fold [12]. Despite these clear oral delivery challenges, few alternate formulation strategies have been reported for AbA [13]. These strategies include the development of an Ab HCl monohydrate salt [14], nanoamorphous AbA preparation by continuous flow precipitation [11,15,16] and the application of SoluMatrix Fine Particle technology [17–19]. However, research is yet to be published on the application of an effective LBF strategy for AbA, expected to be highly beneficial due to its lipophilicity and significant food effect.

In the current study, we apply the super-SLH formulation approach to the clinically relevant compound, AbA. The influence of AbA supersaturation level and type of lipid on physicochemical and in vitro performance were investigated. The in vitro dissolution and drug solubilization during lipolysis were investigated to assess the amount of drug in the molecular state available for absorption compared to the commercial product. The extent of digestion over time and the chemical nature of glycerides and free fatty acids (FA) were elucidated by ^{1}H NMR analysis to gain insight into the mechanisms of action of super-SLH. This information has the potential to be used in the development of an AbA loaded super-SLH formulation for use in humans to improve patient compliance and performance.

MATERIALS AND METHODS

Materials

Abiraterone acetate (AbA) and abiraterone (Ab) were purchased from Hangzhou Dayangchem Co. Ltd. (Hangzhou City, China). Zytiga tablets were purchased from the Royal Adelaide Hospital (Adelaide, Australia) and crushed into a uniform powder before use, to allow for direct comparison to the SLH powder and so that a dose smaller than 250 mg could be dosed in vitro. Capmul PG8 and Capmul MCM were donated by Abitec (Columbus, USA). Parteck SLC 500, porous silica microparticles with a diameter of 9–11 μm and pore size of 6 nm [20], was donated by Merck Millipore (Bayswater, Australia). Phenacetin, coumarin 6, rhodamine B, tris maleate, sodium taurodeoxycholate, sodium hydroxide (NaOH) pellets, calcium chloride dihydrate, 4-bromophenyl boronic acid, formic acid and L-α-phosphatidylcholine (from dried egg yolk, >40% enzyme) were purchased from Sigma Aldrich (Castle Hill, Australia).

Pancreatin was purchased from MP Biomedicals (Seven Hill, Australia). Sodium chloride, hydrochloric acid (HCl), acetonitrile, propan-2-ol, methanol, chloroform deuterated chloroform and dichloromethane were purchased from Chem Supply (Gillman, Australia). High purity Milli-Q water (Merck Millipore, Bayswater, Australia) was used throughout the study.

Liquid Chromatography-Mass Spectrometry (LCMS)

A Shimadzu LCMS 8030 (Kyoto, Japan) and a Phenomenex Kinetex C-18 (50 × 3 mm, 2.6 μm particle size) column (Torrance, USA) were used to determine unknown concentrations of AbA and Ab, using phenacetin as an internal standard. Ion detection was performed in multiple reaction monitoring mode and positive ion mode. The mass transitions for AbA, Ab and phenacetin were *m/z* 392.2/332.25, *m/z* 350.1/156.15, and *m/z* 180.0/110.1, respectively. A gradient elution at a flow rate of 0.4 mL/min was employed, including mobile phase A (0.1% formic acid in water (*v/v*)) and mobile phase B (0.1% formic acid in acetonitrile (*v/v*)) with a run time of 5.1 min. The time program of the gradient method was set as mobile phase B 20% (0.5 min), 80% (3.5–4.5 min), and 20% (4.6–5.1 min). The column oven was maintained at 40°C and the injection volume was 1 μL.

Solubility of AbA in Lipids and Aqueous Media

Capmul PG8 and Capmul MCM were chosen for their high AbA solubilizing capabilities and different digestion rates and extents. Capmul PG8 exhibits rapid and incomplete digestion while Capmul MCM exhibits gradual and complete digestion (see Fig. S6). AbA solubility in lipid was determined at 25, 37 and 60°C. Excess AbA was added to a centrifuge tube containing approximately 500 mg of lipid. The tube was vortex mixed for 20 s, sonicated for 5 min and placed on a rotator for 24 h in an oven maintained at the required temperature. The undissolved drug was separated from the supernatant by centrifugation for the measurements at 25°C and 37°C (37,560 *g*, 20 min, 25 or 37°C) and by gravity for the measurements at 60°C. A 10 mg portion of lipid supernatant was weighed into a fresh tube with 1 mL of acetonitrile and sonicated for 30 min to extract AbA from the lipid. The tube was centrifuged (37,560 *g*, 20 min, 25°C) and the supernatant was diluted appropriately with acetonitrile and spiked with internal standard prior to LCMS analysis. The original tube was vortex mixed to redisperse the pellet and was returned to the rotator for a further 24 h. This method was repeated until a S_{eq} was reached, i.e. a less than 10% difference compared to the previous assay.

The solubility of AbA was also determined in 0.1 M HCl and fasted state micelles (see section 2.10.1) at 37°C. Excess AbA was added to a centrifuge tube containing 500 μL of media. The tube was vortex mixed for 20 s, sonicated for 5 min and placed on a rotator for 24 h in an oven maintained at 37°C. The undissolved drug was separated from the supernatant by centrifugation (37,560 *g*, 20 min, 37°C). The supernatant was diluted appropriately with acetonitrile and spiked with internal standard prior to LCMS analysis. The original tube was vortex mixed to redisperse the pellet and returned to the rotator for a further 24 h. This method was repeated until a S_{eq} was reached.

Fabrication of Super-SLH

The fabrication of super-SLH was based on a previously established method [5]. AbA and lipid were weighed into glass vials and heated to 60°C in an oven for approximately 1–2 h with intermittent shaking to dissolve the AbA. Porous silica was added directly into the vials containing the hot lipid/drug and immediately mixed with a spatula to promote the imbibition of the lipid/drug into the silica pores to obtain a white dry stable super-SLH powder. The silica:lipid ratio was maintained at 1:1 *w*/w. The AbA was loaded at 4 different drug loads in relation to the AbA S_{eq} in the lipid at 25°C, i.e. 90% S_{eq} (SLH) and 150, 200 and 250% S_{eq} (super-SLH).

Determination of Drug Load

Solvent extraction was performed to extract the AbA from the SLH and super SLH formulations, followed by LCMS analysis to determine the drug loading. Approximately 10 mg of each formulation was weighed into a glass vial to which 10 mL of acetonitrile was added. The contents of the vial were sonicated for 30 min to extract the AbA. A 500 μL sample was removed from the vial and centrifuged (37,560 *g*, 20 min, 25°C) to separate any undissolved material. The supernatants containing the extracted AbA in acetonitrile were appropriately diluted and spiked with internal standard prior to analysis by LCMS.

Solid-State Characterisation

The physical state of AbA loaded within the formulations was assessed for crystallinity using x-ray powder diffraction (XRPD). XRPD patterns were obtained using a Malvern Panalytical Empyrean XRPD (Malvern, UK) with θ – θ geometry. Samples were scanned between 5° and 50° (2θ) at a rate of 5 s/point and step size of 0.02°. Measurements were performed at 1 and 14 days after super-SLH fabrication to assess the short-term physical stability.

Scanning Electron Microscopy

Scanning electron microscopy was performed on a Carl Zeiss Merlin microscope with a GEMINI II column (Jena,

Germany) to examine the surface morphology of the formulations. Samples were held in place using double sided adhesive carbon tape and were sputter coated with 10 nm platinum prior to imaging at an accelerating voltage of 2 kV.

Confocal Imaging

Confocal laser scanning microscopy was performed on a Zeiss Elyra PS-1 microscope (Jena, Germany) for super-SLH before and after undergoing 60 min of lipolysis (on the dried pellet), by labelling the porous silica and lipids with rhodamine B and coumarin 6, respectively. Confocal images were captured at the emission wavelength of 488 nm for coumarin 6 (excitation wavelength 497 nm) and 625 nm for rhodamine B (excitation wavelength 540 nm).

In Vitro Dissolution

AbA dissolution studies comparing SLH, super-SLH, pure AbA and Zytiga were performed in 0.1 M HCl solution (pH 2), as AbA is reported to be practically insoluble in aqueous media over a broad range of pH values [2–12], however slightly soluble in 0.1 M HCl solution [21]. Dissolution was performed in 450 mL of media using a USP II apparatus maintained at 37°C and rotating at 50 rpm. Quantities of formulation equivalent to 20 mg of AbA were added. 5 mL aliquots were removed from the vessels over 60 min, subjected to a 0.45 μm syringe filter and diluted appropriately with acetonitrile and spiked with internal standard prior to LCMS analysis. The aliquots were replaced with fresh media.

In Vitro Lipolysis

Preparation of Simulated Intestinal Media

Fasted and fed state mixed micellar solutions with a bile salt: phosphatidylcholine concentration of 5:1.25 mM and 20: 5 mM, respectively, were prepared according to a method adapted from [22]. Egg lecithin was dissolved in chloroform, followed by the evaporation of chloroform under vacuum to achieve a thin film of lecithin in a round bottom flask (Büchi Rotavapor RE, Flawil, Switzerland). NaTDC (bile salt) and standard lipolysis buffer (pH 7.5, containing 50 mM tris maleate, 150 mM sodium chloride and 5 mM calcium chloride dihydrate) were added and stirred overnight to obtain a transparent micellar solution.

Digestion Experimental Procedure

Pancreatin extract (containing pancreatic lipase, colipase and other nonspecific lipolytic enzymes and proteins) was prepared fresh daily by stirring 2 g of pancreatin in 10 mL of standard lipolysis buffer for 15 min, followed by centrifugation (8450 *g*, 20 min, 4°C). The supernatant was collected and refrigerated until required. Lipid digestion kinetics were monitored for 60 min using a Metrohm 902 Titrando pH-stat titration apparatus equipped with a Dosino 800 dosing apparatus (Herisau, Switzerland). Prior to initiating each lipolysis experiment, 18 mL of mixed micellar medium were equilibrated to 37°C in a thermostated glass vessel, and pH adjusted to 7.50 ± 0.05 using 0.5 M NaOH or 0.5 M HCl. For each lipolysis experiment, an amount of formulation equivalent to 3 mg of AbA was added. This amount of AbA corresponded to a concentration 3-fold greater than the AbA S_{eq} in fasted state mixed micelles. The formulation was allowed to disperse in the equilibrated digestion medium for 1 min and the pH was re-adjusted to 7.5. Lipolysis was initiated by the addition of 2 mL pancreatin extract. FA produced during digestion were immediately titrated with 0.6 M NaOH to maintain a constant pH of 7.50 ± 0.01 in the digestion medium. The cumulative volume of NaOH was converted to the moles of FA released and used to compare the rate and extent of lipid digestion for the different formulations using the equation below, where the cumulative volume of NaOH (corrected for the volume of NaOH needed for background lipolysis of blank micellar solutions) is multiplied by the NaOH concentration and the molar ratio of NaOH:FA:

$$n_{FA} = [V_{NaOH\ Formulation} - V_{NaOH\ Blank}][C_{NaOH}] \quad (1)$$

Drug Phase Partitioning

The distribution (quantities) of AbA in the aqueous phase and pellet during in vitro lipolysis were investigated. Sample aliquots (1 mL) were withdrawn at 1, 5, 15, 30, 45 and 60 min and collected into 1.5 mL centrifuge tubes prepared with 10 μL of 4-bromophenyl boronic acid (0.5 M in methanol) to inhibit lipase activity. Samples were centrifuged (21,130 *g*, 10 min, 25°C) to separate the aqueous phase, containing solubilized AbA, and pellet, containing precipitated drug. The supernatant was appropriately diluted and spiked with internal standard prior to analysis by LCMS. The pellet was isolated and re-dispersed through addition of 1 mL acetonitrile, vortex mixing for 30 s followed by sonication for 20 min. The tube was centrifuged (21,130 *g*, 10 min, 25°C) and the supernatant was appropriately diluted and spiked with internal standard prior to analysis by LCMS.

Lipid Phase Partitioning

The partitioning of lipid species between the aqueous and pellet phases after in vitro lipolysis was determined by coupling proton nuclear magnetic resonance (^{1}H NMR) spectroscopy and thermogravimetric analysis (TGA), as shown

previously [23]. Lipolysis aliquots (2 mL) were centrifuged at 29,060 *g* for 5 min to separate the aqueous and pellet phases. The aqueous phase was subjected to a liquid-liquid extraction with dichloromethane (6 mL), followed by evaporation at room temperature using a Buchi Rotavapor RE (Flawil, Switzerland) and resuspension in deuterated chloroform. ^{1}H NMR spectra was obtained using a Bruker Ultrashield 500 (Billerica, USA) with the following acquisition parameters: spectral width 6410 Hz, relaxation delay 3 s, number of scans 64, acquisition time 4.819 s, pulse width 90°. Lipid species (diglycerides (DG), monoglycerides (MG), FA and monoesters) were quantified as previously described [24–26].

To determine the phase partitioning of lipid species, one half of the lipolysis pellet was dried at 40°C for 3 h and kept in a desiccator overnight. The dried lipolysis sample was subjected to TGA using a TA Instruments Discovery TGA (New Castle, USA) to quantify the lipid content in the pellet. Samples were heated at a scanning rate of 10°C/min from room temperature to 60°C, under nitrogen purge. Lipid components completely decompose within the temperature range 150°C – 400°C, while silica remains stable. The phase partitioning of lipid species was calculated by coupling the mass of lipid present in the pellet (determined with TGA) with the relative concentration of lipid species in the pellet (determined by ^{1}H NMR). It was assumed that the mass of lipid in the aqueous phase was equal to the difference between the initial mass and mass in the pellet [23].

Statistical Analysis

Statistically significant differences were determined by one-way analysis of variance followed by Tukey's post-test for multiple comparisons using GraphPad Prism v 8.3.0 (GraphPad Software, San Diego, USA). Values are reported as the mean ± standard deviation (SD), and the data were considered statistically significant when $p < 0.05$.

RESULTS

Temperature Dependent Solubility of AbA in Lipids

Solubility studies were performed at 25, 37 and 60°C in Capmul PG8 and Capmul MCM to assess the ability for the lipids to supersaturate AbA (Fig. 1A). AbA solubility in both lipids increased linearly with temperature (Fig. 1B). AbA solubility in Capmul PG8 was 65, 38 and 11% greater than in Capmul MCM at 25, 37 and 60°C, respectively. At 60°C, compared to 25°C, solubility was enhanced 2.1- and 3.1-fold in Capmul PG8 and Capmul MCM, respectively.

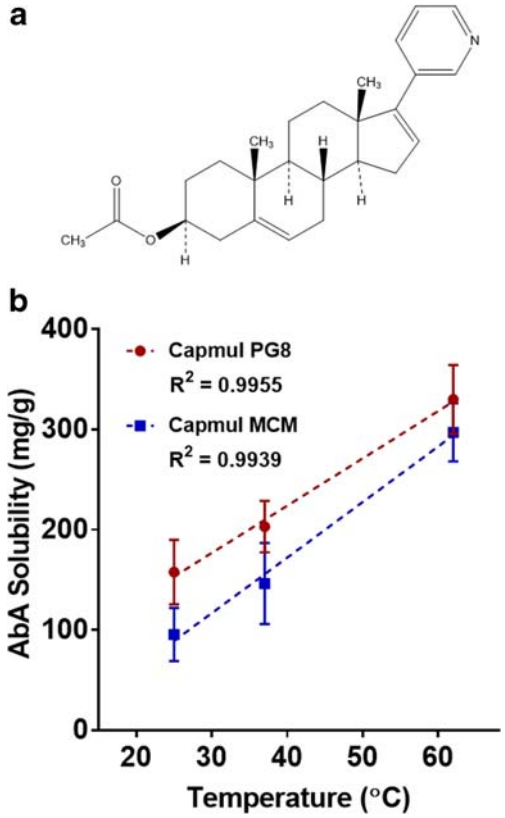

Fig. 1 (A) The chemical structure of AbA. (B) The temperature dependent solubility of AbA in Capmul PG8 and Capmul MCM. Data represents mean ± SD, $n = 3$.

Super-SLH Preparation and Characterisation

Super-SLH and SLH (not supersaturated) were successfully prepared, forming white flowing powders. The formulations and their compositions are summarized in Table I. The AbA loaded super-SLH were found to have an approximate 100% drug loading efficiency. Crushed Zytiga tablets (containing 250 mg AbA) were found to contain 34.6 ± 1.6% *w*/w AbA, in agreement with the labelled drug content, i.e. 99.4%.

Drug Crystallinity and Stability

XRPD was utilized to qualitatively characterize the solid state of the AbA within the super-SLH formulations. Unformulated crystalline AbA exhibited a characteristic XRPD pattern as reported in literature (Fig. 2A) [27]. When diluted with porous silica to form a physical mixture, the XRPD pattern of AbA was not visible at an AbA concentration of 1% w/w, however this was visible at 5% w/w (Fig. S1A). Therefore, the limit of detection of the XRPD for AbA lies between 1 and 5% w/w, which is sufficient to detect the lowest drug loads associated with non-saturated SLH, which range from 4.8–6.2% w/w. The SLH P90, super-SLH P150, P200 and P250 were prepared and analysed by XRPD after 1 (Fig. 2B) and 14 days (Fig. S1C) of storage in an airtight glass vial at room

Table I The composition of the fabricated SLH formulations

Lipid Type	Formulation Name	Saturation Level (% S_{eq})	Drug Load (% w/w)	Lipid Load (% w/w)	Silica Load (% w/w)
Capmul PG8	SLH P	–	0	50.0	50.0
	SLH P90	90	6.2	46.9	46.9
	Super-SLH P150	150	10.0	45.0	45.0
	Super-SLH P200	200	12.8	43.6	43.6
	Super-SLH P250	250	15.6	42.2	42.2
Capmul MCM	SLH M	–	0	50.0	50.0
	SLH M90	90	4.8	47.6	47.6
	Super-SLH M150	150	7.8	46.1	46.1
	Super-SLH M200	200	10.2	44.9	44.9
	Super-SLH M250	250	12.4	87.6	87.6

temperature. No AbA peaks were visible for SLH P90 and super-SLH P150, suggesting that the drug was non-crystalline, whereas super-SLH P200 and P250 displayed small scattered peaks suggesting some crystalline material was present. The XRP diffractograms matched those reported in literature for AbA [27] and not those of known AbA polymorphs [28]. Furthermore, after 14 days of storage, there were no obvious differences in the peaks of the formulations suggesting stability for a minimum of 14 days. All experiments were conducted using super-SLH and SLH within 1 week of preparation.

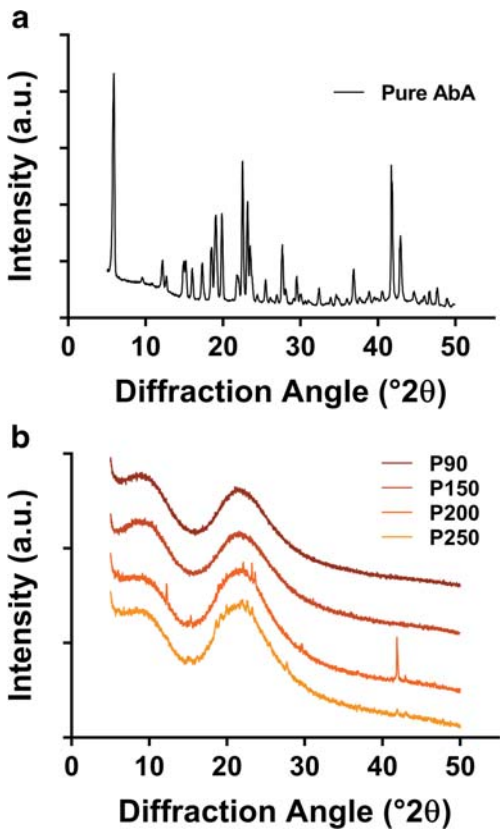

Fig. 2 XRP diffractograms of (A) unformulated crystalline AbA and (B) SLH P90, super-SLH P150, P200 and P250 after 1 day of storage.

Super-SLH and SLH formulations made with Capmul MCM were not investigated with XRPD since there was no statistical difference observed in the solubilisation capacity between PG8 and MCM ($p > 0.05$).

Surface Morphology

The surface morphology of each formulation was analyzed by scanning electron microscopy (SEM) (Fig. 3). The unformulated AbA appeared as large crystalline plate-like structures with diameters ranging from 10 to 160 μm (Fig. 3A). The blank silica particles appeared as irregular structures ranging in diameter from 5 to 20 μm with smaller fragments scattered on the surface (Fig. 3B). No visual differences were observed with regard to the surface morphology and structure of super-SLH formulations, compared to the blank silica particles, irrespective of the lipid used or supersaturation level (Fig. 3C and S2).

Lipid Distribution in SLH

The distribution of fluorescently labelled lipid within the porous silica microparticles was investigated by confocal microscopy (Fig. 4). For SLH P, the majority of lipid was observed on the outside of the particles with less lipid imbibed within in the silica pores. After 60 min of lipolysis, little lipid remained on the surface or within the particles. In contrast, lipid was homogenously dispersed throughout the porous network of SLH M, with some additional lipid located between the inter-particle cavities. After 60 min of lipolysis, no lipid could be observed between adjoined silica particles, while lipid remained homogenously dispersed throughout the porous silica.

In Vitro Dissolution

The dissolution performance of the SLH, super-SLH, Zytiga and pure AbA are compared in Fig. 5. Pure

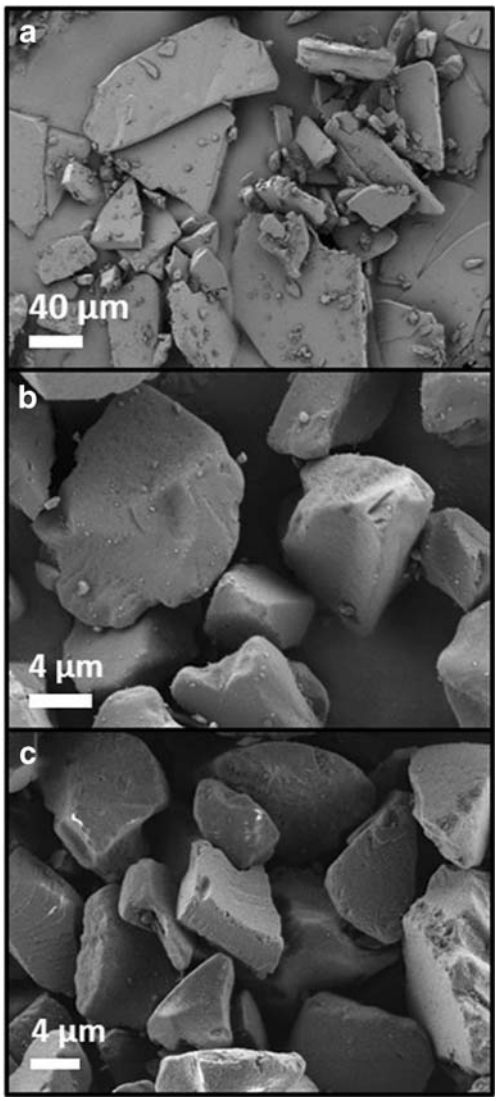

Fig. 3 SEM images of (A) unformulated crystalline AbA, (B) blank silica microparticles and (C) super-SLH P250 (representative of all (super-)SLH formulations shown in Fig. S2).

AbA and Zytiga, achieved 4% and 27% solubilization after 60 min, respectively. Super-SLH P significantly enhanced AbA solubilization, achieving 56–68% after 60 min. This was 2–2.5-fold greater than Zytiga and 16–19-fold greater than pure AbA ($p < 0.05$). The only statistical significance between the different SLH P drug loads was between SLH P90 and super-SLH P200 ($p < 0.05$).

Conversely, super-SLH M did not enhance AbA solubilization, achieving just 9–14% solubilization after 60 min. The solubilization of super-SLH M was not significantly greater than pure AbA ($p > 0.05$) and was a significantly less than Zytiga ($p < 0.05$). There was no statistical significance between the performance of the different super-SLH M drug loads. Thus, super-SLH P performed significantly greater than super-SLH M ($p < 0.05$).

In Vitro Lipolysis and Solubilization

Aqueous Drug Solubilization

The partitioning of AbA between the aqueous phase and pellet was measured over a 60 min lipolysis period. The percentage recovery for AbA ranged from 80 to 120% at all time points and for each formulation, as displayed in Fig. S3 and S4. Small discrepancies in drug recovery (i.e. recovery ≠ 100%) can be explained by poor separation of the pellet from the aqueous phase, either by losing some of the pellet or not removing the entire aqueous phase from the pellet before dilution and analysis.

AbA and Ab were both measured simultaneously throughout the lipolysis studies due to the potential for AbA to be hydrolysed to Ab in the intestinal media containing pancreatin [29]. However, after the 60 min lipolysis period, there was ≤5% Ab present and so was considered negligible.

The concentration-time profiles of solubilized AbA in the aqueous phase during fasted state in vitro lipolysis studies, under simulated intestinal conditions, are presented in Fig. 6A and B. For pure AbA and Zytiga, the level of drug solubilization gradually increased over the 60 min lipolysis period to reach 7% and 30%, respectively. The rate of drug solubilization from all SLH/super-SLH formulations was initially rapid with a subsequent plateau or slow increments in drug solubilization after 5 min. All SLH and super-SLH significantly enhanced the extent of solubilization of AbA compared to pure AbA, while only SLH P90 demonstrated significantly greater drug solubilization than Zytiga at after 60 min ($p < 0.05$). In contrast, all SLH showed a significantly greater cumulative drug solubilization (area under the solubilisation-time curve, AUC_{sol}) than Zytiga ($p < 0.05$).

SLH P90 and super-SLH P150, P200 and P250 achieved 83, 44, 40 and 43% AbA solubilization in the aqueous phase after 60 min, respectively, whereas SLH M90 and super-SLH M150 achieved 52 and 46%. The performance of SLH P90 was significantly enhanced compared to all other formulations ($p < 0.05$), and no significance was found between the different super-SLH ($p > 0.05$). All SLH and super-SLH achieved AbA concentrations above the equilibrium solubility of AbA in the media (48.5 ± 3.2 µg/mL), whereas pure AbA and Zytiga did not. Based on these findings, super-SLH M200 and M250 were not investigated further as they were expected to exhibit poorer performance than SLH M90 and super-SLH M150.

Following addition of blank SLH P with super-SLH P250 to achieve an equivalent lipid dose to SLH P90 (Fig. 7A) the solubilization of AbA slightly increased, however not significantly compared to super-SLH P250 alone ($p > 0.05$) and did not reach the AbA solubilization level of SLH P90.

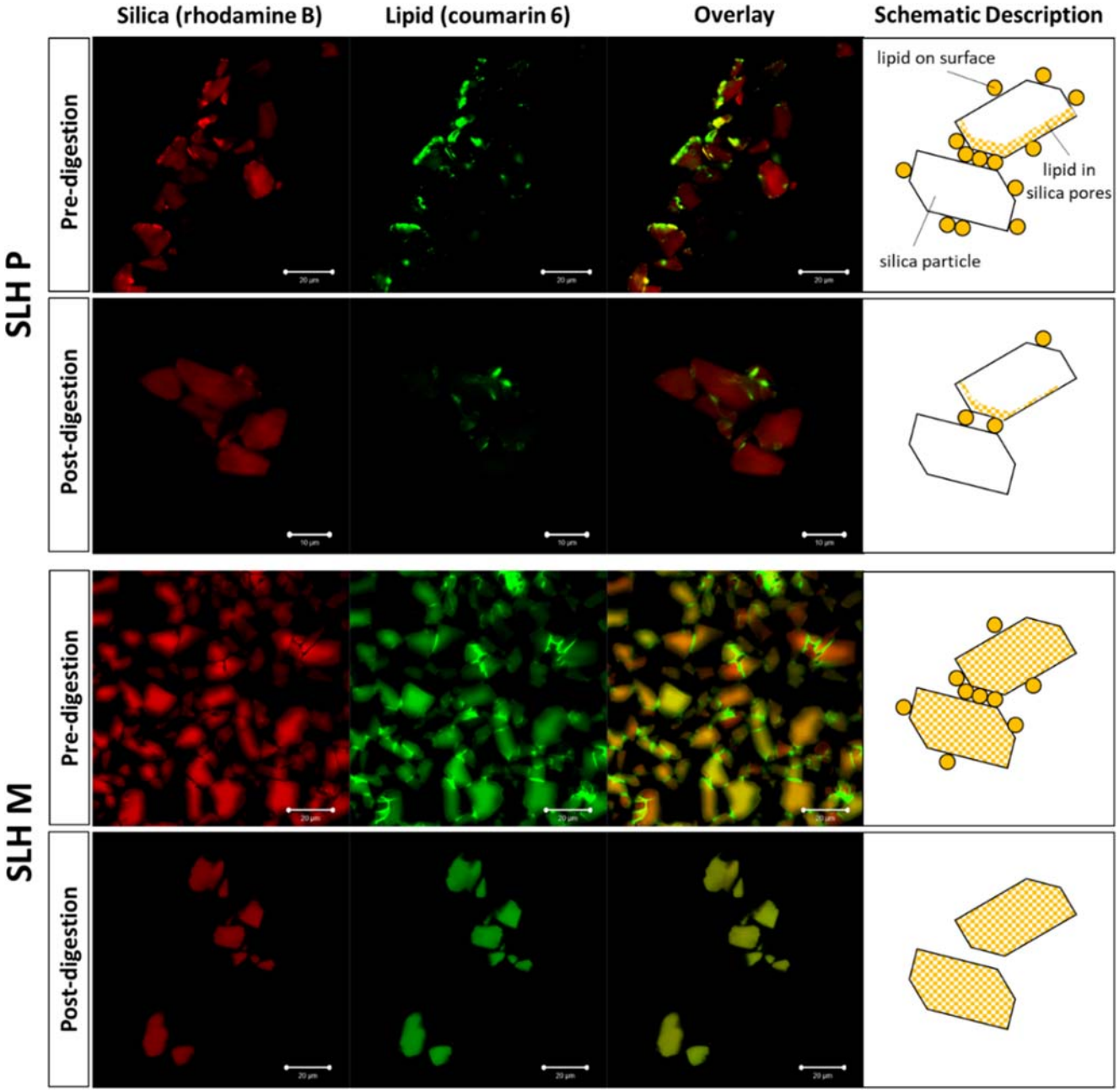

Fig. 4 Confocal images of blank SLH P and SLH M before and after 60 min of digestion. The silica was labelled with rhodamine B (red), while the lipid was labelled with coumarin 6 (green).

Lipid Digestion and Speciation

The lipid digestion-time profiles for the SLH and super-SLH are displayed in Fig. 6C and D**.** With an increase in drug load, there was a decrease in the extent of digestion after 60 min. It is important to note that the lipid dose was not controlled in the study (lipid dose ranged from 8 to 30 mg), as SLH and super-SLH were dosed based on their drug load to provide a constant drug dose rather than constant lipid dose. There was a positive correlation ($R^2 = 0.9252$) between the amount of lipid dosed and the extent of digestion of the super-SLH after 60 min, as expected (Fig. S5). Pure AbA and Zytiga did not exhibit any digestion (data not shown) and the lipid digestion of Capmul PG8 and Capmul MCM were not compromised when loaded into silica (Fig. S6). The chemical nature and quantity of glycerides and FA's released to the aqueous phase after the 60 min lipolysis period were elucidated by ^{1}H NMR spectra in combination with TGA (Fig. 8A). The aqueous phases of SLH P and SLH M at the completion of the lipolysis period contained 82% and 59% of the dosed lipid, respectively. The digestion products for SLH P and SLH M were 5.2% DG, 9.3% MG and 68.0% FA/monoesters, and 3.3% DG,

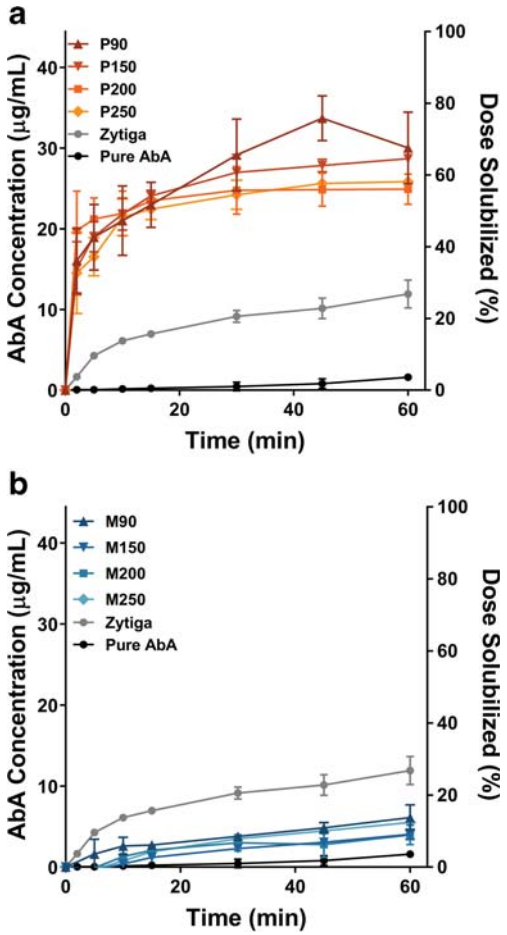

Fig. 5 The dissolution-time profiles of (A) SLH/super-SLH P and (B) SLH/super-SLH M, at various saturation levels, dosed at 20 mg AbA to 450 mL 0.1 M HCl solution maintained at 37°C (non-sink). Data represents mean ± SD, n = 3.

12.2% MG and 33.2% FA/monoesters, respectively. The reference ^{1}H NMR spectra of lipid species present in the pellets are included in Fig. S7.

When super-SLH P250 was co-dosed with blank super-SLH P to achieve an equivalent lipid dose to SLH P90 (Fig. 7B), the degree of lipid digestion in the vessel after 60 min was significantly enhanced 2.2-fold **($p > 0.05$)**, yet not to the same extent as SLH P90.

Influence of the Fed State on Drug Solubilization

The concentration-time profiles of solubilized AbA in the fasted state were compared to the fed state, under simulated intestinal conditions (Fig. 9). Zytiga was compared to SLH P90 as it displayed the greatest extent of solubilization during in vitro lipolysis studies. For Zytiga, after 60 min of lipolysis in the fed state, 95% of AbA was solubilized in the aqueous phase, compared to 30% in the fasted state. The AUC_{sol} for these profiles were 6018 ± 176 and 1999 ± 74 µg/mL/min, demonstrating a significant 3-fold fed-fasted-state variability **($p < 0.05$)**. For SLH P90, after 60 min of lipolysis in the fed state, 88% of AbA was solubilized in the aqueous phase, compared to 83% in the fasted state. The AUC_{sol} for these profiles were 7768 ± 305 and 6630 ± 250 µg/mL/min, demonstrating a significant, yet relatively minor 1.17-fold fed-fasted-state variability **($p > 0.05$)**.

DISCUSSION

The aim of this study was to develop a supersaturated solid-state LBF of AbA that (i) increases drug loading and solubilization efficiency compared to the commercial product Zytiga, and (ii) achieves fed-fasted state equivalence. This study, to the best of our knowledge, is the first application of a LBF to AbA, and the first application of a BCS Class IV PWSD to the super-SLH formulation.

Super-SLH, which is comprised of lipids confined within porous silica microparticles, was selected as the carrier system for AbA due to its already proven ability to stabilize supersaturated PWSDs in the molecular state [5]. That is, the dual mechanism of medium-chain length lipids, such as Capmul PG8 and Capmul MCM, which possess high solubilizing capacities of poorly water soluble drugs [30,31], in combination with porous silica that has demonstrated ability to stabilize drugs in an amorphous state on its surface and within its pores [6,20,32], providing a multifaceted approach to stabilizing the supersaturated state of encapsulated drug molecules. Supersaturated loading of AbA within SLH was achieved by heating the lipid and drug to 60°C to allow AbA solubilization at a saturation level greater than possible in lipid at room temperature, followed by subsequent stabilization with porous silica microparticles. Since excessive supersaturation of LBF can lead to drug recrystallization and a non-optimal in vitro and in vivo performance [5,8], super-SLH drug loading levels of 150, 200 and 250% S_{eq} were investigated and compared to non-supersaturated SLH (90% S_{eq}).

SLH and super-SLH were able to maintain AbA in the molecular/non-crystalline state at saturation levels of 90 and 150% S_{eq}, however at 200 and 250% S_{eq} a small portion of the AbA had recrystallized. This was likely due to the supersaturated drug load exceeding the silica and lipids ability to stabilize the drug in an amorphous state. The relative intensity of the crystalline AbA peaks within the XRP diffractogram of super-SLH P200 and P250, compared to the controls, suggest that the crystalline content was approximately 3–4 and 2–3% *w*/w respectively, which represents approximately one quarter of their drug loads. This is in agreement with the previous study where super-SLH containing ibuprofen displayed an increasing amount of crystalline drug with an increase in drug loading [5], and therefore, 150% supersaturation can be considered the optimal saturation level to maximise AbA load, while maintaining the entire drug load in an amorphous state.

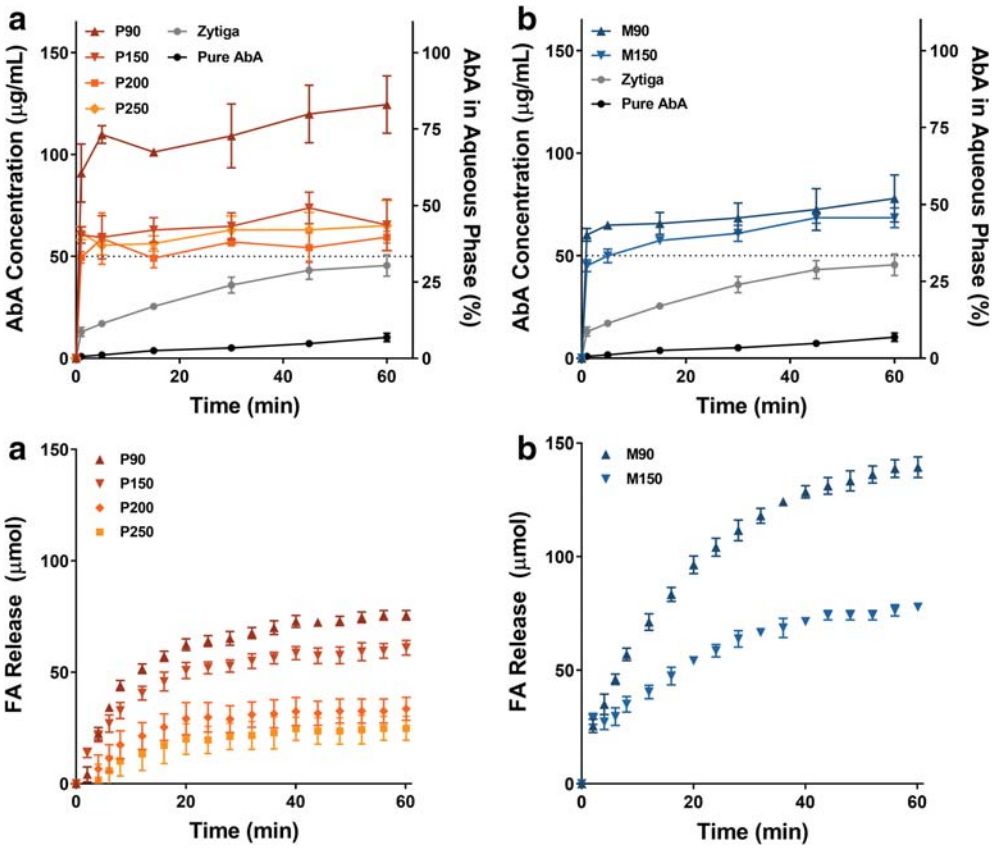

Fig. 6 The concentration-time profiles and digestion-time profiles of AbA, from (A and C) SLH and super-SLH P and (B and D) SLH and super-SLH M, in the aqueous phase after a 3 mg AbA dose of formulation under biorelevant fasted digesting conditions. Dotted line represents the AbA S_{eq} in the fasted-state media. Data represents mean ± SD, n = 3.

AbA dissolution kinetics were impacted by the solid-state and particle size of AbA within the investigated formulations. When drug is maintained in the molecular state within LBF, the rate-limiting step of dissolution is removed, and rapid dissolution is achieved [33]. Whereas, when drug is crystalline, the dissolution rate is directly proportional to the surface area of the drug, which increases with decreasing particle size. Therefore, pure crystalline AbA particles exhibited poor dissolution due to its large particle size (10–160 μm), while Zytiga displayed improved dissolution due to its reduced particle size (micronized AbA, 3–10 μm) and solubilizing excipients (sodium lauryl sulfate) [11]. Furthermore, the SLH and super-SLH prepared using Capmul PG8 provided rapid dissolution of AbA due to most of the drug load being maintained in its molecular state, achieving extents of dissolution greater than Zytiga. In contrast, SLH and super-SLH prepared with Capmul MCM did not achieve dissolution extents greater than Zytiga, this is considered due to the lipids different abilities to maintain the drug in the molecular state and their relative affinity and distribution in the silica particles (as discussed in depth later).

The lack of biorelevance of the dissolution medium (i.e. absence of digestive enzymes, lack of solubilisation species, such as bile salts, and low pH)limited the interpretation of drug release and solubilization from LBF [34], thus solubilization was monitored during in vitro lipolysis studies. In contrast to dissolution studies, during lipolysis, all SLH and super-SLH formulations, regardless of the lipid type, achieved greater extents of solubilization than Zytiga. Lipolysis demonstrated LBF's major advantage over Zytiga; that is, the ability for its exogenous lipid excipients to be digested and promoting drug release, while maintaining drug solubilization within the lipophilic environment generated by the lipid digestion products [35]. The study also provided greater discrimination between the different drug loaded SLH and super-SLH formulations. These differences were highly influenced by drug load, where higher saturation levels resulted in lower solubilization levels, thought to be due to the increasing crystalline content (limiting dissolution) and/or reduced relative concentration of co-dosed lipid with respect to drug content (limiting solubilization capacity during digestion). To investigate this further, lipolysis was performed to determine whether maintaining an equivalent lipid to drug ratio would trigger equivalent drug solubilisation between SLH P90 and super-SLH P250. This was achieved by dosing extra lipid in the digestion media (in the form of blank SLH P) with super-SLH P250 during lipolysis. Interestingly, the lipid digestion and drug solubilization achieved by super-SLH P250 + blank SLH P were still significantly less than SLH P90. This suggests that the digestibility of the formulation is critical to drug release/solubilization, as

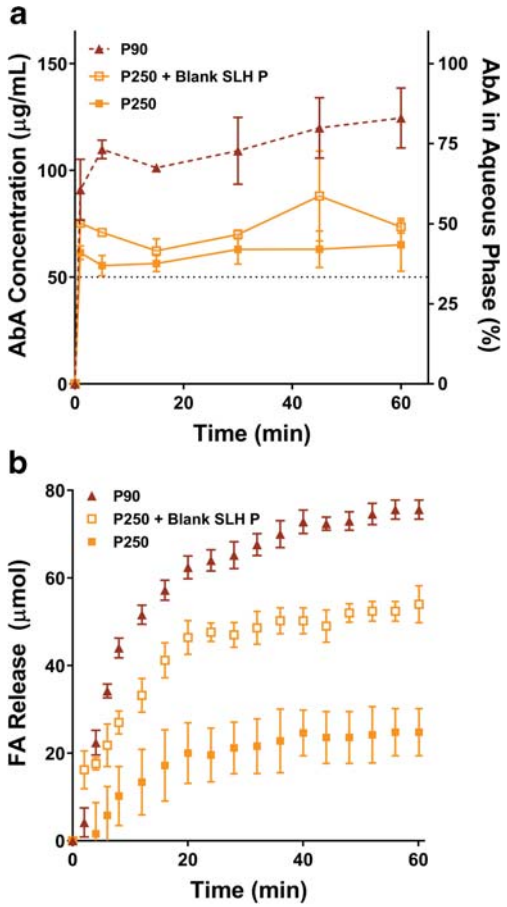

Fig. 7 The (A) concentration-time profiles and (B) digestion-time profiles of AbA solubilization, from super-SLH P250 and super-SLH P250 with additional blank SLH P to equivalate the lipid dose of SLH P90, in the aqueous phase after a 3 mg AbA dose of formulation under biorelevant fasted digesting conditions. Dotted line represents the AbA S_{eq} in the fasted-state media. Data represents mean ± SD, n = 3.

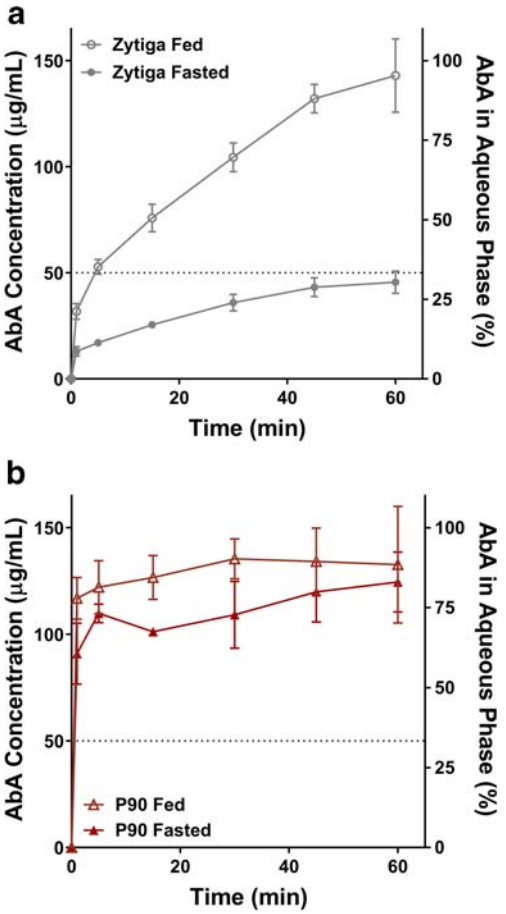

Fig. 9 The concentration-time profiles of AbA solubilization, from (A) Zytiga and (B) SLH P90, in the aqueous phase over 60 min after a 3 mg AbA dose of formulation under biorelevant fasted and fed digesting conditions. Dotted line represents the AbA S_{eq} in the fasted-state media. Data represents mean ± SD, n = 3.

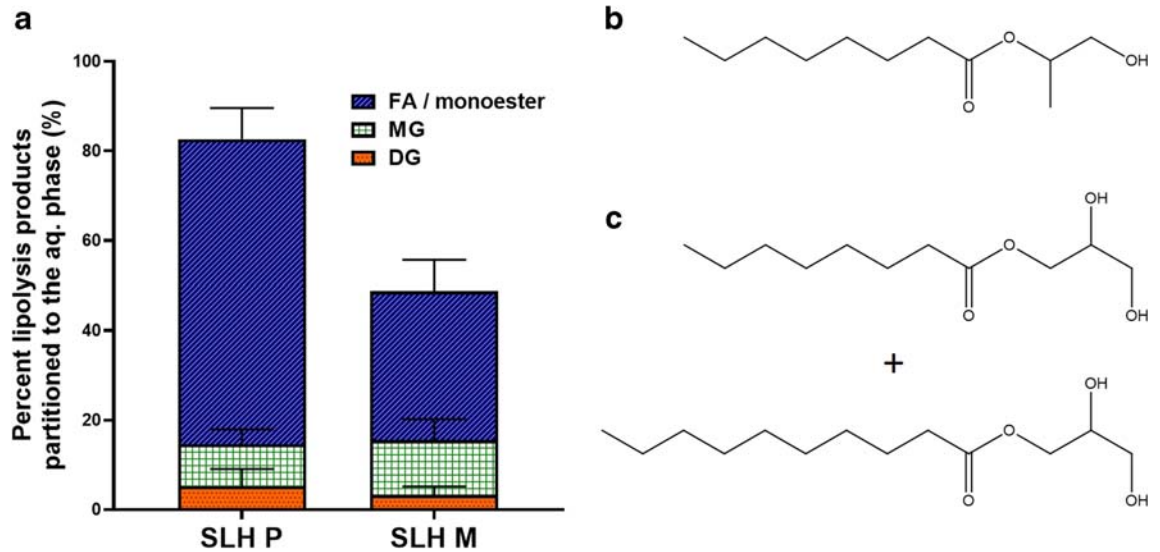

Fig. 8 (A) The speciation of the lipid digestion products in the aqueous phase, of SLH P and SLH M after 60 min of digestion. Data represents mean ± SD, *n* = 3. The chemical structures of (B) Capmul PG8 (monoester of caprylic acid) and (C) Capmul MCM (mixture of MG and DG of caprylic and capric acids, DG not shown).

SLH P90 demonstrates good digestibility and drug release. The amount of lipid, lipid digestibility and the digestion products released from the formulations, also appears to have an impact. This is further demonstrated by the performance of super-SLH P150, which did not appear to contain any crystalline AbA, as per XRPD analysis, however behaves similarly to P200 and P250 in digestion experiments. Solubilization extent was not only influenced by drug load, due to differences in crystalline drug content, but it was also dependent on the type of lipid employed to prepare super-SLH. That is, the solubilisation capacity of SLH formulations prepared with Capmul PG8 was significantly greater at all saturation levels, compared to those prepared with Capmul MCM, which can be attributed to the difference in chemical structure of the lipids and the physical adsorption mechanisms of the lipid to the silica. Capmul PG8 (propylene glycol monocaprylate; Fig. 8B) is a monoester of caprylic acid with a composition of ≥90% propylene glycol monoesters and a FA distribution of ≥90% caprylic acid. In contrast, Capmul MCM (glyceryl caprylate/caprate; Fig. 8C) is a mixture of mono and diglycerides, with a composition of 45–75% monoglycerides, 20–50% diglycerides and < 10% triglycerides, with a FA distribution of 10–50% capric acid and 50–90% caprylic acid [36]. The 2 lipids presented different distributions within the SLH, as shown by the confocal images, however it is not yet clear why this occurred. When SLH was fabricated using Capmul PG8, it adsorbed to the outside of the silica particles with minimal lipid entering the pores. Upon digestion, the lipid was readily accessible to the hydrolytic enzymes present in the lipolysis media, liberating 82% of the lipid into the aqueous phase and leaving little Capmul PG8 remaining on the surface or within the particles. Subsequently, the lipid in the aqueous phase contained a large portion of FA. In contrast, when SLH was fabricated using Capmul MCM, the lipid was homogenously dispersed throughout the porous silica network, with some additional lipid located between the inter particle cavities. During digestion, the lipid between the inter particle cavities was completely digested and liberated from the silica surface, leading to 59% of the lipid being released into the aqueous phase, while a large degree of lipid remained confined within the porous network of the silica particles (Fig. 10). This can be attributed to the high DG and MG content of Capmul MCM, since previous studies have highlighted that only the FA portion of lipid digestion products are expelled from within silica pores during lipolysis, due to electrostatic repulsion [24,37]. Therefore, only the minor portion of DG and MG that was digested, forming FA, partitioned towards the aqueous phase, while the neutral charge DG and MG remained within the silica pores.

Since it was presumed that AbA was co-localized with the lipid during lipolysis, the increase in aqueous partitioning of digestion products for SLH P was considered a driving force for the increase in AbA aqueous solubilization, when compared to SLH M. The higher relative lipid concentration within the aqueous phase from the digestion of SLH P, compared to SLH M, allowed for greater AbA solubilization in micellar structures and vesicles containing bile salts, phospholipids, DG, MG and FA **[**23**]**. Meanwhile, the retained Capmul MCM glycerides were expected to have retained AbA within the silica. It is important to note the limitation of the lipolysis study, whereby that the concentration of lipid digestion products within the lipolysis media likely exceeds that which would be present in the gastrointestinal tract, due to the low volume used in this study. Subsequently, the degree of fasted-state solubilization may exceed that expected in vivo [38,39]. The final objective of this study was to elucidate whether formulating AbA with SLH could reduce its fed-fasted state variability. The principle cause of positive food effects exhibited by PWSDs, such as AbA, is their lack of solubility and dissolution in the fasted state in comparison to the fed state. This is a result of dramatic changes in the physicochemical composition of the gastrointestinal fluid that occur after the administration of a meal [40,41]. The presence of dietary lipids (as little as 2 g) in the duodenum stimulate the secretion of bile salts, phospholipids and cholesterol from the gall bladder and pancreatic fluids and lipases from the pancreas [7]. These species generate a range of colloidal structures including micelles, mixed micelles, vesicles and emulsion droplets that provide lipidic microenvironments into which co-administered PWSDs may partition into, maintaining their solubilization and promoting enhanced drug absorption [35,42]. The in vitro lipolysis experiments were performed in simulated fed state intestinal media and compared to the fasted state. Remarkably, Zytiga displayed a significant 3-fold increase in in vitro solubilization in the fed state, whereas SLH P90 displayed no significant difference. This is in agreement with a significant 5 to 10-fold food effect measured in humans [12]. The variability displayed by Zytiga is owing to containing microcrystalline AbA that exhibits enhanced solubilization capacity in the more lipophilic fed state. Whereas, SLH P90 mitigates the fed-fasted variability due to the AbA being pre-solubilized within the lipid, essentially mimicking the positive food effect. LBFs are well recognized for their potential to reduce the impact of food on drug absorption, with minimal lipid being able to mimic the food effect for many drugs [7,43–45]. By maximizing dissolution in the fasted state, LBF can also prevent these postprandial increases in solubilization and mitigate or even eliminate the positive food effect [40]. However, due to the inability to simulate the complete and complex physiological processes associated with digestion in vitro (e.g. ingestion, gastric digestion and emptying), it is difficult to fully predict the effect of the super-SLH formulation on mitigating the food effect of AbA [29,46,47]. Subsequently, well-designed and systematic in vivo studies are required to fully validate the potential of super-SLH in mitigating the food effect of AbA. Further, studies in an

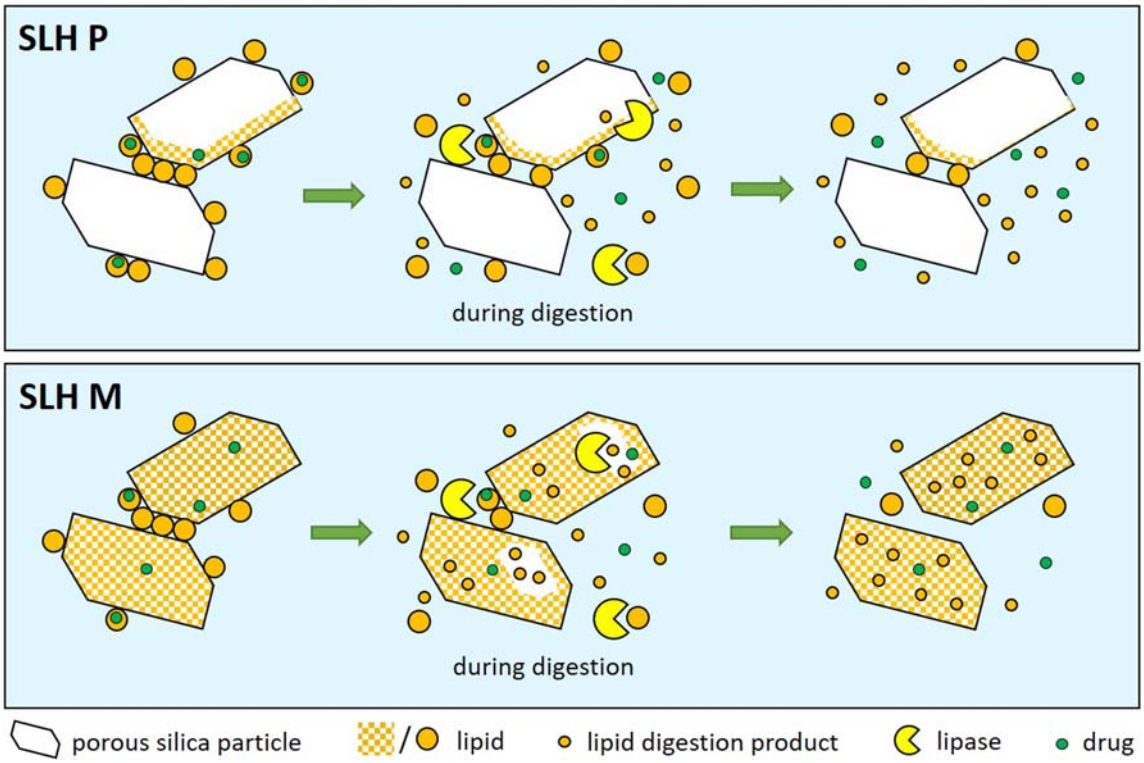

Fig. 10 A schematic of the lipolysis and AbA solubilizing mechanisms of SLH.

animal model, such as beagle dogs, could confirm if this in vitro observation can be translated in vivo to remove the need for fasting when administering AbA [12]. As other oral formulation strategies for AbA have shown strong in vitro-in vivo correlations resulting in significant oral bioavailability enhancement and mitigation of the food effect compared to Zytiga [11,17], SLH also has the potential to translate its in vitro benefits in vivo.

This work demonstrates the ability of SLH and super-SLH to overcome the oral delivery challenges associated with Zytiga. The findings suggest that for super-SLH, and for all supersaturated LBF, there is a fine balance between achieving high drug loads using supersaturation (to reduce formulation dose) and improving performance using the LBF approach (to reduce drug dose). In the case of AbA, supersaturation in lipid compromised solubilization performance, which is in contrast to the previous study employing super-SLH for ibuprofen, where drug solubilization and in vivo performance was maintained up to a saturation level of 227% S_{eq}. This suggests that the effect of super-SLH may be drug dependent and further studies into the application of super-SLH for other PWSDs are needed to determine these effects more broadly.

Super-SLH have the potential to improve the patient compliance of those prescribed AbA, through food-independent dosing and reduction of pill burden by finding the optimal balance between supersaturated drug loads and enhanced solubilization for promoting absorption. In considering the feasibility of clinical dosing AbA via super-SLH, we note that at a 10% *w*/w AbA load, and based on achieving a 3.5-fold improvement in oral bioavailability (which is feasible based on our in vitro data), the required AbA dose could be reduced to 285 mg, enabling an equivalent amount of super-SLH formulation to be dosed as Zytiga (i.e. ~2.9 g). In addition to the benefit of a reduced drug dose there is the potential for no restrictions on food administered with the drug.

Compared to other PWSD enabling formulation strategies, super-SLH uses a simple yet scalable manufacturing process. Other strategies such as amorphous solid dispersions or nano-sized preparations may require specialist equipment such as spray dryers, extruders, granulators or homogenizers. However, the limitations of the super-SLH formulation including its drug loading and formulation dose need to be further optimized for clinical translation.

Future work should focus on the refinement of the delivery system to optimize the potential benefits to the patient and their translation in vivo.

CONCLUSIONS

The SLH and super-SLH formulation approaches were successfully applied to AbA and enhanced the extent of drug solubilization during in vitro lipolysis. The 2 key factors that influenced AbA solubilization from super-SLH were (i) the saturation level of AbA, which in turn determined the solid state of AbA and the relative amount of lipid, and (ii) the lipid

utilized, which in turn determined the degree of digestion of the formulation and the affinity of the lipid and lipid digestion products to the silica. While all saturation levels of SLH significantly improved the lipolysis-mediated solubilization of AbA compared to Zytiga, the greatest solubilization was achieved by SLH P90, the non-supersaturated SLH formulated with Capmul PG8, owing to completely non-crystalline/molecular AbA being co-dosed with the greatest amount of lipid. SLH P90 also exhibited negligible fed-fasted state variability, in contrast to the a 3-fold difference observed for Zytiga. The presented in vitro data demonstrates the fine balance between achieving high drug loads using supersaturation and improving performance using the LBF approach. These findings support the further investigation into the in vivo pharmacokinetic performance of super-SLH for AbA, and thus, drive the pre-clinical development of an alternative oral formulation to Zytiga with greater efficiency and an eliminated food effect.

Acknowledgements and Disclosures. The Australian Government Research Training Program is acknowledged for the PhD Scholarship of Hayley Schultz. Funding was provided by the Gould Experimental Science Grant. This work was performed in part at the South Australian node of the Australian National Fabrication Facility under the National Collaborative Research Infrastructure Strategy.

REFERENCES

1. Feeney OM, Crum MF, McEvoy CL, Trevaskis NL, Williams HD, Pouton CW, et al. 50 years of oral lipid-based formulations: provenance, progress and future perspectives. Adv Drug Deliv Rev. 2016;101:167–94.
2. Tang B, Cheng G, Gu J-C, Xu C-H. Development of solid self-emulsifying drug delivery systems: preparation techniques and dosage forms. Drug Discov Today. 2008;13(13–14):606–12.
3. Mandić J, Pobirk AZ, Vrečer F, Gašperlin M. Overview of solidification techniques for self-emulsifying drug delivery systems from industrial perspective. Int J Pharm. 2017;533(2):335–45.
4. Joyce P, Dening TJ, Meola T, Schultz H, Holm R, Thomas N, et al. Solidification to improve the biopharmaceutical performance of SEDDS: opportunities and challenges. Adv Drug Deliv Rev. 2019;142:102–17.
5. Schultz HB, Thomas N, Rao S, Prestidge CA. Supersaturated silica-lipid hybrids (super-SLH): an improved solid-state lipid-based oral drug delivery system with enhanced drug loading. Eur J Pharm Biopharm. 2018;125:13–20.
6. McCarthy CA, Ahern RJ, Dontireddy R, Ryan KB, Crean AM. Mesoporous silica formulation strategies for drug dissolution enhancement: a review. Expert Opinion on Drug Delivery. 2016;13(1):93–108.
7. Kossena GA, Charman WN, Wilson CG, O'Mahony B, Lindsay B, Hempenstall JM, et al. Low dose lipid formulations: effects on gastric emptying and biliary secretion. Pharm Res. 2007;24(11):2084–96.
8. Schultz HB, Kovalainen M, Peressin KF, Thomas N, Prestidge CA. Supersaturated silica-lipid hybrid (super-SLH) oral drug delivery systems: balancing drug loading and in vivo performance. J Pharmacol Exp Ther. 2019;370(3):742–50.
9. Tan A, Eskandar NG, Rao S, Prestidge CA. First in man bioavailability and tolerability studies of a silica–lipid hybrid (Lipoceramic) formulation: a phase I study with ibuprofen. Drug Delivery and Translational Research. 2014;4(3):212–21.
10. Hoy SM. Abiraterone acetate: a review of its use in patients with metastatic castration-resistant prostate cancer. Drugs. 2013;73(18):2077–91.
11. Solymosi T, Ötvös Z, Angi R, Ordasi B, Jordán T, Semsey S, et al. Development of an abiraterone acetate formulation with improved oral bioavailability guided by absorption modeling based on in vitro dissolution and permeability measurements. Int J Pharm. 2017;532(1):427–34.
12. Chi KN, Spratlin J, Kollmannsberger C, North S, Pankras C, Gonzalez M, et al. Food effects on abiraterone pharmacokinetics in healthy subjects and patients with metastatic castration-resistant prostate cancer. J Clin Pharmacol. 2015;55(12):1406–14.
13. Schultz HB, Meola TR, Thomas N, Prestidge CA. Oral formulation strategies to improve the bioavailability and mitigate the food effect of abiraterone acetate. International Journal of Pharmaceutics. 2020; (under review). [Journal Article].
14. Silveira RG, Cunha BN, Tenório JC, de Aguiar DVA, da Cruz SP, Vaz BG, et al. A simple alternative to prodrug: the hydrochloride salt monohydrate of the prostate anticancer drug abiraterone. J Mol Struct. 2019;1190:165–70.
15. Solymosi T, Ötvös Z, Angi R, Ordasi B, Jordán T, Molnár L, et al. Novel formulation of abiraterone acetate might allow significant dose reduction and eliminates substantial positive food effect. Cancer Chemother Pharmacol. 2017;80(4):723–8.
16. Basa-Dénes O, Solymosi T, Ötvös Z, Angi R, Ujhelyi A, Jordán T, et al. Investigations of the mechanism behind the rapid absorption of nano-amorphous abiraterone acetate. Eur J Pharm Sci. 2019;129:79–86.
17. Goldwater R, Hussaini A, Bosch B, Nemeth P. Comparison of a novel formulation of abiraterone acetate vs. the originator formulation in healthy male subjects: two randomized, open-label, crossover studies. Clin Pharmacokinet. 2017;56(7):803–13.
18. Papangelou A, Olszanski AJ, Stein CA, Bosch B, Nemeth P. The effect of food on the absorption of abiraterone acetate from a fine particle dosage form: a randomized crossover trial in healthy volunteers. Oncology and Therapy. 2017;5(2):161–70.
19. Stein CA, Levin R, Given R, Higano CS, Nemeth P, Bosch B, et al. Randomized Phase 2 therapeutic equivalence study of abiraterone acetate fine particle formulation vs. originator abiraterone acetate in patients with metastatic castration-resistant prostate cancer: The STAAR study. Urologic Oncology: Seminars and Original Investigations. 2018;36(2):81 e89–81. e16.
20. Kissi EO, Ruggiero MT, Hempel N-J, Song Z, Grohganz H, Rades T, et al. Characterising glass transition temperatures and glass dynamics in mesoporous silica-based amorphous drugs. Phys Chem Chem Phys. 2019;21(35):19686–94.
21. FDA CDER, NDA 202–379 review – abiraterone acetate, 2010, Available from: https://www.accessdata.fda.gov/drugsatfda_docs/nda/2011/202379orig1s000clinpharmr.pdf [Report].
22. Sek L, Porter CJ, Kaukonen AM, Charman WN. Evaluation of the in-vitro digestion profiles of long and medium chain glycerides and the phase behaviour of their lipolytic products. J Pharm Pharmacol. 2002;54(1):29–41.
23. Dening TJ, Joyce P, Prestidge CA. Improving correlations between drug solubilization and in vitro lipolysis by monitoring the phase partitioning of lipolytic species for lipid-based formulations. J Pharm Sci. 2019;108(1):295–304.

24. Joyce P, Barnes TJ, Boyd BJ, Prestidge CA. Porous nanostructure controls kinetics, disposition and self-assembly structure of lipid digestion products. RSC Adv. 2016;6(82):78385–95.
25. Joyce P, Gustafsson H, Prestidge CA. Enhancing the lipase-mediated bioaccessibility of omega-3 fatty acids by microencapsulation of fish oil droplets within porous silica particles. J Funct Foods. 2018;47:491–502.
26. Dening TJ, Joyce P, Rao S, Thomas N, Prestidge CA. Nanostructured montmorillonite clay for controlling the lipase-mediated digestion of medium chain triglycerides. ACS Appl Mater Interfaces. 2016;8(48):32732–42.
27. Solymosi T, Tóth F, Orosz J, Basa-Dénes O, Angi R, Jordán T, et al. Solubility measurements at 296 and 310 K and physicochemical characterization of abiraterone and abiraterone acetate. J Chem Eng Data. 2018;63(12):4453–8.
28. Polymorphs of Abiraterone Acetate and Preparation Method Thereof. CN101768199 A, 2010. [Patent].
29. Stappaerts J, Geboers S, Snoeys J, Brouwers J, Tack J, Annaert P, et al. Rapid conversion of the ester prodrug abiraterone acetate results in intestinal supersaturation and enhanced absorption of abiraterone: in vitro, rat in situ and human in vivo studies. Eur J Pharm Biopharm. 2015;90:1–7.
30. Porter CJH, Kaukonen AM, Taillardat-Bertschinger A, Boyd BJ, O'Connor JM, Edwards GA, et al. Use of in vitro lipid digestion data to explain the in vivo performance of triglyceride-based oral lipid formulations of poorly water-soluble drugs: studies with halofantrine. J Pharm Sci. 2004;93(5):1110–21.
31. Koehl NJ, Holm R, Kuentz M, Griffin BT. New insights into using lipid based suspensions for 'brick dust' molecules: case study of nilotinib. Pharm Res. 2019;36(4):56.
32. Choudhari Y, Reddy U, Monsuur F, Pauly T, Hoefer H, McCarthy W. Comparative evaluation of porous silica based carriers for lipids and liquid drug formulations. Open Material Sciences. 2014;1(1):61–74.
33. Meola TR, Dening TJ, Prestidge CA. Nanocrystal-silica-lipid hybrid particles for the improved oral delivery of ziprasidone in vitro. Eur J Pharm Biopharm. 2018;129:145–53.
34. Klein S. The use of biorelevant dissolution media to forecast the in vivo performance of a drug. AAPS J. 2010;12(3):397–406.
35. Porter CJ, Pouton CW, Cuine JF, Charman WN. Enhancing intestinal drug solubilisation using lipid-based delivery systems. Adv Drug Deliv Rev. 2008;60(6):673–91.
36. Abitec Corporation. Oral brochure. 2019. Available from: https://www.abiteccorp.com/en/pharmaceutical/pharmaceutical-dosage-forms/oral/. [Brochure].
37. Joyce P, Tan A, Whitby CP, Prestidge CA. The role of porous nanostructure in controlling lipase-mediated digestion of lipid loaded into silica particles. Langmuir. 2014;30(10):2779–88.
38. Kazi M, Alanazi FK, Hussain MD. In vitro methods for in vitro-in vivo correlation (IVIVC) for poorly water soluble drugs: lipid based formulation perspective. Current Drug Delivery. 2018;15(7):918–29.
39. Williams HD, Anby MU, Sassene P, Kleberg K, Bakala-N'Goma J-C, Calderone M, Jannin V, Igonin A, Partheil A, Marchaud D, Jule E, Vertommen J, Maio M, Blundell R, Benameur H, Carrière F, Müllertz A, Pouton CW, Porter CJH. Toward the establishment of standardized in vitro tests for lipid-based formulations. 2. the effect of bile salt concentration and drug loading on the performance of type I, II, IIIA, IIIB, and IV formulations during in vitro digestion. Molecular Pharmaceutics. 2012;9(11):3286–3300.
40. O'Shea JP, Holm R, O'Driscoll CM, Griffin BT. Food for thought: formulating away the food effect – a PEARRL review. J Pharm Pharmacol. 2019;71(4):510–35.
41. Pentafragka C, Symillides M, McAllister M, Dressman J, Vertzoni M, Reppas C. The impact of food intake on the luminal environment and performance of oral drug products with a view to in vitro and in silico simulations: a PEARRL review. J Pharm Pharmacol. 2019;71(4):557–80.
42. Wiedmann TS, Kamel L. Examination of the solubilization of drugs by bile salt micelles. J Pharm Sci. 2002;91(8):1743–64.
43. Christiansen ML, Holm R, Kristensen J, Kreilgaard M, Jacobsen J, Abrahamsson B, et al. Cinnarizine food-effects in beagle dogs can be avoided by administration in a self nano emulsifying drug delivery system (SNEDDS). Eur J Pharm Sci. 2014;57:164–72.
44. Tan A, Martin A, Nguyen T. Hung, Boyd BJ, Prestidge CA. Hybrid nanomaterials that mimic the food effect: controlling enzymatic digestion for enhanced oral drug absorption. Angew Chem. 2012;124(22):5571–5.
45. Thomas N, Holm R, Müllertz A, Rades T. In vitro and in vivo performance of novel supersaturated self-nanoemulsifying drug delivery systems (super-SNEDDS). J Control Release. 2012;160(1):25–32.
46. Geboers S, Stappaerts J, Mols R, Snoeys J, Tack J, Annaert P, et al. The effect of food on the intraluminal behavior of abiraterone acetate in man. J Pharm Sci. 2016;105(9):2974–81.
47. Koziolek M, Carrière F, Porter CJH. Lipids in the stomach – implications for the evaluation of food effects on oral drug absorption. Pharm Res. 2018;35(3):55.